A Climatology of Turbulent Dispersion in the Troposphere

MATTHEW HUBER

Department of Earth Sciences, University of California, Santa Cruz, Santa Cruz, California

JAMES C. MCWILLIAMS AND MICHAEL GHIL

Department of Atmospheric Sciences and Institute of Geophysics and Planetary Physics, University of California, Los Angeles, Los Angeles, California

(Manuscript received 7 April 2000, in final form 2 November 2000)

ABSTRACT

The authors present properties of turbulent, meridional mixing along isentropic surfaces within the troposphere. Twice-daily wind fields analyses from the European Centre for Medium-Range Weather Forecasts numerical weather prediction model for 1992 are used to calculate Lagrangian trajectories of large ensembles of particles. The ensemble-averaged rms growth of the meridional relative dispersion over the first 10 days after particle release is used to quantify mixing properties. These properties are considered as a function of height in the atmosphere, season, and geographic region. Results are characterized by release latitude and flow regime and compared with simple theories.

All three dispersive regimes—exponential, ballistic, and Richardson–Obukhov—that have been documented in previous studies are found to be important. The extratropics are found to display superdiffusive growth of the relative rms dispersion, consistent with the nonlocal character of midlatitude mixing. The Tropics are characterized by exponential growth of the rms dispersion, consistent with locally constant eddy timescales. Some evidence for zonal inhomogeneity in dispersion growth rates is found.

1. Introduction

The atmosphere's large-scale circulation causes mixing of tracer particles and air masses. This mixing, or lack thereof, is believed to play an important role in many atmospheric phenomena: in the theory of global water-vapor distribution (Kelly et al. 1991; Yang and Pierrehumbert 1994), in explaining the prerequisite chemical isolation for polar ozone-hole formation (Leovy et al. 1985), in paleoclimate temperature reconstructions from tracer-derived proxy data (Joussaume and Jouzel 1993), in predicting meridional heat fluxes (e.g., Held 1999), and in considering potential vorticity (PV) as an active rather than a passive tracer in planetary circulations (Haynes and McIntyre 1987; Hoskins 1991). The characterization of mixing is therefore crucial in guiding and validating theories and models of the atmospheric general circulation.

One approach to characterize mixing and transport is to calculate Lagrangian trajectories for passive tracers in ''realistic'' atmospheric flows. Our goal in this study is to characterize tropospheric mixing properties as a function of geographic location, height, and season in a way that is easily compared to previous analyses. We focus solely on mixing in the meridional direction. We do so with the most realistic wind fields available, those derived from analyses of atmospheric data using the European Centre for Medium-Range Weather Forecasts (ECMWF) model. In order to obtain results that are statistically robust we have chosen a sampling strategy of large ensembles from a wide variety of initial release locations. A reasonable simplifying approximation in doing so is that air motions are adiabatic, so particle trajectories may be calculated along isentropic surfaces. This limits the validity of our analysis to a relatively short interval of a few to 10 days, as discussed below. This study fills the gap between better understood, idealized, strictly two-dimensional (2D) mixing and more realistic, but largely unexplored, fully three-dimensional (3D) atmospheric mixing.

We discuss the historical background of this problem and issues that remain unresolved by previous studies in the next section. The data and the analysis methods are presented in section 3. The dispersion behavior using the ECMWF winds is reported in section 4. The main results are summarized and implications for the large-scale atmospheric circulation are discussed in section 5.

Corresponding author address: Matthew Huber, Earth Sciences Dept., University of California, Santa Cruz, Santa Cruz, CA 95064. E-mail: mhuber@es.ucsc.edu

2. History and unresolved issues

Lagrangian parcel-trajectory analysis has been used extensively for synoptic studies of the troposphere on the one hand and for the elucidation of large-scale stratospheric dynamics on the other. The latter studies have taken advantage of the nearly 2D character of stratospheric flows. In fact, with the significant exception of motions in which diabatic forcing is important (e.g., in the tropical troposphere) large-scale tropospheric flows may also be approximated as quasi-horizontal and hence nearly 2D. Therefore, features of 2D and quasigeostrophic (i.e., nearly 2D) turbulence theory have been utilized as reference models to compare against observed aspects of geophysical turbulence. The existence of k^{-3} horizontal wind spectra near the tropopause (e.g., Nastrom and Gage 1985), as predicted by both 2D (Fjørtoft 1953) and quasigeostrophic (Charney 1971) turbulence theory, supports the relevance of these simplified models.

Various simple computational models of 2D flow have been developed to investigate aspects of mixing and stirring phenomena in geophysical fluids. Useful simplifications have included idealized domains, stretching mechanisms, or flow configurations (Basdevant et al. 1981; Aref 1983; McWilliams 1984; Pierrehumbert 1991a, b; Weiss 1991; Young and Jones 1991; Jones 1991; Maltrud and Vallis 1991; Babiano et al. 1994; Rom-Kedar and Paldor 1997; Weiss et al. 1998). These studies have advanced the paradigm of transport and mixing by chaotic advection (Rom-Kedar et al. 1990; Aref 1991; Wiggins 1992). In this study, we utilize the concepts of *transport*, the transfer of substance from one macroscopic region to another, and *mixing regions*, which are bounded by transport barriers of varying degrees of impermeability, that have been developed by previous authors.

The relatively simple picture of chaotic advection in 2D flows is made more complex by the inclusion of multiple mixing mechanisms (e.g., transient eddies, Rossby waves, and jets) as well as by the presence of possible transport barriers, such as at the tropopause and the equator. It remains unclear so far how these complicating factors may affect overall atmospheric mixing and transport, since their effects have proven difficult to model analytically or by using simple computational or experimental models. Much work has focused therefore on detailed observations and numerical models of the geophysical fluids themselves. The behavior of passive tracers tracked with Lagrangian methods has proven to be a useful diagnostic tool for this purpose. Several statistical measures of the separation of Lagrangian particles have been found useful in characterizing the turbulent flow regimes; these include correlation functions (Pierrehumbert 1991a,b), finite-time Lyapunov exponents (Pierrehumbert 1991a,b), and relative dispersion (Richardson 1926; Richardson and Stommel 1948; Maryon and Buckland 1995).

In this study, we will utilize the relative dispersion,

$$K_r(t) = \frac{1}{2}\frac{d\sigma_r^2(t)}{dt}. \tag{1}$$

The rms distance $\sigma_r(t)$ between particles is defined relative to the average position of a particle,

$$\sigma_r(t) = \langle [x(t) - \overline{x}(t)]^2 \rangle^{1/2}, \tag{2}$$

where $\langle\ \rangle$ denotes an average over all particle releases and the overbar denotes the average over a single puff of particles. All distances and growth rates in this study refer to only the meridional separation of particles. As discussed by Er-El and Peskin (1981), for the purposes of studies such as our own, a relative measure is preferable to a single-particle estimate of the diffusivity (e.g., Thiébaux 1976) due to the Galilean invariance of the former.

With an ensemble approach, we gain the ability to assess the statistical reliability of our dispersion laws and thereby better characterize the mixing that any particular atmospheric region is usually subject to. But this comes at the expense of losing the ability to relate the mixing properties to time-varying events. Hence, we compare our time-averaged dispersion against the time-averaged wind fields with the understanding that much of the useful information pertaining to individual synoptic events is lost. The relative dispersion that we use is well suited for comparison with results in other turbulence studies (discussed below).

In stationary, homogenous turbulence, after a sufficient time has passed for all initial correlations to vanish, $\sigma_r(t)$ grows as $t^{1/2}$ (Richardson 1926). More generally, there are a number of theoretical considerations (e.g., Frisch 1995; Provenzale 1999, and references therein) that suggest a power-law behavior. In particular, the presence of velocity correlations at shorter times, such as those produced by coherent structures, may alter the power-law exponent γ so that in general, we may write

$$\sigma_r(t) \sim t^{\gamma}. \tag{3}$$

Dispersion with $\gamma < 1/2$ is termed subdiffusive, and $\gamma > 1/2$ is superdiffusive; the particular case of $\gamma = 1$ is ballistic, and that of $\gamma = 1.5$ is the Richardson–Obukhov (RO) law.

Superdiffusivity can occur due to the presence of rapid, long ''flights'' of particles (Solomon et al. 1994), such as those that may be produced by strong large-scale shear (Young and Jones 1991). The ballistic law arises from persistent Lagrangian correlations, and it also has been justified as an effect of nonergodicity due to the coexistence of regular and chaotic regions in 2D incompressible flows (Mezic and Wiggins 1994; del-Castillo-Negrete 1998). The RO law can be obtained in 2D flow from assuming that particles have lost the memory of their initial separation, while the correlations of relative accelerations are stationary (Babiano et al. 1990). Results of simple scaling arguments (Batchelor 1952; Babiano et al. 1990) identify the RO law as oc-

curring when the relative particle separation is of the order of the length scale of energy-cascade eddies, that is, eddies with a spatial scale smaller than ~200 km in the atmosphere (Nastrom and Gage 1985). Subdiffusive behavior is often attributed to the presence of ''trapping'' within eddies (Cardoso et al. 1996) or invariant tori (Behringer et al. 1991; Provenzale 1999).

In Hamiltonian systems theory, the presence of anomalous dispersion, that is, dispersion characterized by $\gamma \neq 1/2$, has been placed within the context of Lévy walks and fractal space and time (Shlesinger et al. 1993; Provenzale et al. 1995; Klafter et al. 1996; Seo and Bowman 2000). By using (3), which appears in a wide variety of systems (Klafter et al. 1996 and references therein), we facilitate comparison with these results and observational studies (below). Not all theoretical predictions lead to power-law behavior, however. As described below, there is both theoretical and observational evidence for the existence of a regime in which dispersion grows as an exponential function of time rather than as a power law.

A large body of Lagrangian parcel trajectories were collected as part of two major field experiments, EOLE (Morel and Bandeen 1973) and Tropical Wind, Energy Conversion and Reference Level Experiment (TWERLE) (Julian et al. 1977), in which hundreds of balloons were released at ~200 mb in the Southern Hemisphere. From the EOLE study, Morel and Larchevêque (1974) deduced that the dispersion process was homogenous, isotropic, and stationary up to horizontal scales of ~1000 km. They demonstrated two regimes of behavior for $\sigma_r(t)$, exponential and diffusive. For timescales less than about 6 days, they found clear evidence of an exponential regime,

$$\sigma_r(t) \sim \sigma_{r_0} e^{t\tau^{-1}}, \tag{4}$$

where τ is a constant timescale. This behavior was derived by Lin (1972) for the 2D enstrophy cascade range (~200–2000 km) and earlier in a different context by Kraichnan (1967), Leith (1968), and Batchelor (1969). Er-El and Peskin (1981) performed a similar analysis of TWERLE; they found that the dispersion was isotropic in both high and low latitudes for roughly the first 6 days and that both high- and low-latitude releases displayed exponential dispersion for times less than about 10 days. Er-El and Peskin (1981) noted, however, that the analysis of EOLE data was flawed because dispersion had been calculated as a simple function of distance rather than being broken into meridional and zonal components. They also concluded that due to the nonstationarity of the data, dispersion should be calculated as a function of time after release rather than distance, and that because of differences in initial flow configuration and sampling size, comparison between distinct field studies is difficult. No error bars on the dispersion or estimates of the goodness of fit were included in Er-El and Peskin (1981). Thus, for example, it is difficult to determine whether the exponential law interpreted by Er-El and Peskin (1981) to hold for 8 to 10 days (their Figs. 4 and 6) may hold instead for 3 to 5 days or whether the midlatitude ''exponential regime'' might not be better fitted by a power law of high order (e.g., $\gamma \geq 1.5$).

Maryon and Buckland (1995) carried out the most realistic long-term, large-scale, numerical simulation of fully 3D atmospheric dispersion to date. These authors deal mostly with midlatitude synoptic-scale mixing effects of single or multiple eddies and not with the spatiotemporal scales dealt with in EOLE and TWERLE. Maryon and Buckland (1995) found that while trapping particles within synoptic-scale eddies causes temporary drops in the rates of dispersion growth in individual release experiments, in general, the dispersion process was a mixture of exponential and superdiffusive growth regimes. As the number of these detailed 3D runs was necessarily small, error bars were not provided, and it remains unclear whether the growth behavior in their superdiffusive regime is ballistic or even stronger.

Pierrehumbert and Yang (1993) performed a study similar to the one described herein, but the wind fields used to drive the dispersion were derived from a general circulation model (GCM) in simulation mode rather than from an analysis of atmospheric observations using a numerical weather prediction model, and the focus was on longer timescales (>10 days). Yang (1995) investigated much more realistic mixing characteristics, although he used comprehensive model results from only a 10-day span in January of a particular year. The methods used in these two studies are similar to those described here, and there are several comparisons that will be discussed below. Using a semi-Lagrangian transport model and ECMWF-derived wind fields projected onto isentropic surfaces, Chen (1995) also analyzed the climatology of tropospheric mixing, but that study's focus was on extratropical cross-tropopause mixing only.

Previous studies have laid out the major ideas and methods of investigation to characterize large-scale dispersion, but there are a number of important unresolved issues.

- The exponential growth law has never been unequivocally identified as a quantitatively better fit than that by a power law. And it is unclear where or for what duration exponential growth should be expected.
- There does not seem to be a consensus as to whether the expected dispersion growth for intermediate time (2–10 days) or large spatial scales (up to hemispheric) should be exponential, ballistic, or the RO law (Babiano et al. 1990; Maryon and Buckland 1995).
- It is also not clear whether the ensemble dispersion should even display just one type of growth on these timescales or a mixture (e.g., Boffetta et al. 1997). The studies just described have found evidence for all three regimes on similar temporal and spatial scales, but it is not clear whether they are contradictory, can-

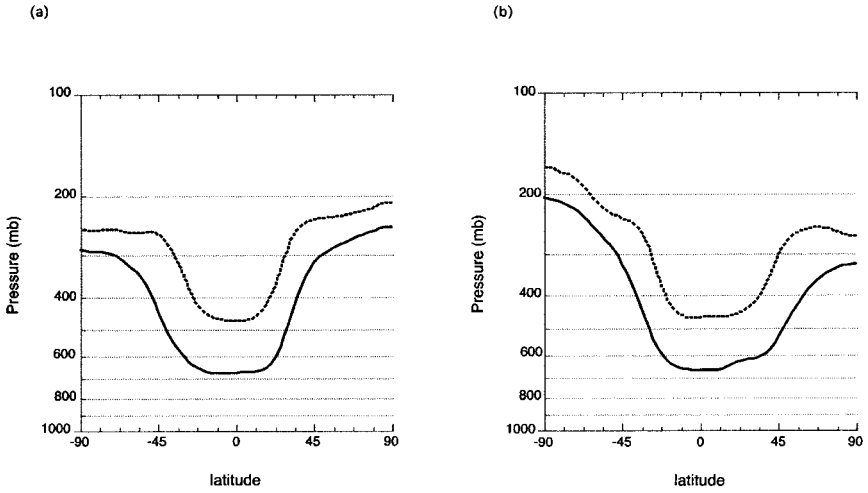

FIG. 1. Zonal-mean, seasonal-average pressure (mb) on the 315-K (solid line) and 330-K (dashed line) isentropic surfaces for boreal (a) winter and (b) summer. Fields are derived from ECMWF model analysis for 1992.

not be compared with each other, or that each reflects only a part of a more complex pattern.

Given these outstanding issues, we are not as optimistic as Babiano et al. (1990), who state that the exponential and RO laws ''have been qualitatively confirmed'' through the observational studies of Morel and Larchevêque (1974). It seems important to resolve these ambiguities in order to relate observed scaling laws to a consistent theory. Coherent structures clearly persist in the atmosphere, despite the action of well-developed turbulence, and significantly affect dispersion. This warrants a careful study of dispersion on a mesoscale to hemispheric scale. No studies have systematically and globally analyzed the key characteristics of climatological tropospheric meridional relative dispersion characteristics according to initial location and height and over a realistic seasonal cycle. By doing so here, we expect to clarify the spatial and temporal variations in dispersion, the degree to which simple theories developed so far actually apply to the real atmosphere, and the conditions under which they do.

3. Data, methods, and sampling strategy

a. Dataset

We interpolate ECMWF analyzed winds onto the two isentropic surfaces at 315 and 330 K for the boreal winter (December, January, February, and March) and summer (June, July, August, and September) of 1992. A puff of 27 nearby particles is released every 12 h into these winds. As shown in Fig. 1, during boreal winter, the 315-K surface resides near 300 mb in the extratropics and near 700 mb in the Tropics, whereas the 330-K surface is closer to 250 and 450 mb, respectively. These are ''middleworld'' (Hoskins 1991) surfaces, which lie definitely within the tropical lower troposphere and rise to somewhere between the upper troposphere and lower stratosphere in the extratropics, depending on definitions of the tropopause.

We chose 72 separate locations as release sources, spaced to sample evenly with respect to area on the sphere. Each puff is initially a circle of particles of diameter 1° on a rectangular latitude–longitude grid. Puffs are released twice daily over a 4-month interval while particle positions and meridional dispersion statistics are calculated. We present an analysis of two distinct sets of 72 separate 4-month integrations extending over the two major seasons. The results of the 72 winter and 72 summer integrations, respectively, have been ensemble averaged in time to produce a statistically meaningful and qualitatively reasonable characterization of the mixing. For a 4-month run, there are about 240 (twice daily) separate releases. Thus, the estimate of $\sigma_r(t)$ for $t = 1$ day involves averaging 239 samples, whereas the estimate for $t = 120$ days would involve only 1 sample. The uncertainty due to sampling error is estimated using the standard error of the scatter in computations of $\sigma_r(t)$ to obtain error bars.

b. Methods and assumptions

The numerical methods used in this study are similar to those in Pierrehumbert and Yang (1993). The fields of horizontal velocity components and temperature $u(x, y, t)$, $v(x, y, t)$, and $T(x, y, t)$, defined at designated pressure levels and with a horizontal resolution of 2.5° × 2.5° in the ECMWF analysis, are interpolated onto isentropic surfaces using bilinear interpolation. Once the 2D isentropic wind fields have thus been generated, a particle trajectory is calculated numerically as the solution to the ordinary differential equations:

$$\frac{dx}{dt} = u(x, y, t), \qquad \frac{dy}{dt} = v(x, y, t), \tag{5}$$

given a time-dependent velocity field (u, v) and an initial position $[x_{(0)}, y_{(0)}] = (x_0, y_0)$.

The temporal resolution necessary for good particle tracking according to Eq. (5) has been estimated to be between 12 (Merril et al. 1986) and 24 h (Pierrehumbert and Yang 1993). This is consistent with the 12-h temporal resolution in this study. We use a fourth-order Runga–Kutta (RK-4) numerical scheme to perform the integration, and although some studies have used higher-order schemes (e.g., Merril et al. 1986), we are confident in the numerical methods we have used for two reasons. First, individual backtrajectories calculated with the RK-4 scheme were validated against observations by comparing them with inferred source locations based on radiosonde measurements of conserved quantities, such as ozone concentration and potential temperature. Second, higher-order integration methods used in other runs produced similar statistics (not shown).

A deficiency of our technique lies in the assumption of adiabaticity. In mid- to high latitudes, the isentropic approximation to parcel motion is accurate for a few to 10 days (e.g., Yang 1995), since diabatic forcing in these regions is weak. In the Tropics, however, both deep convection and strong radiative cooling transport particles across isentropic surfaces. The strongest radiative cooling, usually found in the Tropics, is usually between 1 and 2 K day^{-1} (Sherwood 1996; Pierrehumbert 1998), leading to 10–20 K of cooling over the time interval investigated here. The 15-K separation between the two isentropic surfaces here should allow a fairly accurate representation of real particle trajectories for up to 10 days. Ascent in convecting regions may lead to much higher cross-isentropic velocities, >25 K day^{-1} (Sherwood 1996); therefore, we give more weight to those conclusions that do not rely heavily on the assumption of adiabaticity in the deep Tropics, where the assumption is less valid.

With these caveats, we believe that the isentropic trajectory method used here is justifiable for five distinct and complementary reasons. 1) By considering only the first 10 days of particle travel, systematic errors should be minimized; 2) most of the motions in the atmosphere are roughly adiabatic; 3) vertical velocities in GCMs are not very accurate and frequently do not agree well with available data; 4) comparison with 2D theories and simple models is facilitated; and 5) it is crucial to evaluate the adiabatic circulation's role in dispersion and mixing in order to be understand the effects of the diabatic circulation. Furthermore, it should be remembered that observational studies also investigate purely 2D trajectories, as the balloons travel along constant pressure surfaces. To the degree that motions in the atmosphere are isentropic rather than isobaric, we expect our results to be more representative of real atmospheric mixing.

A smaller problem is that the 315-K surface intersects the ground occasionally in one or two grid boxes over the Himalayas and South Africa. At the particular time and place at which this occurs, we assume continuity of trajectories and choose a wind from a neighboring grid box at the same instant or from the same grid box for the next half day. This heuristic device works well and is not likely to introduce a systematic bias into our results. The 330-K surface has no such intersections, and dispersion on it shows quite similar behavior to the 315-K surface, which lends further credence to our procedure for surface intersections.

c. Spatial and temporal sampling

The Lagrangian methods we apply in this study are able to generate tracer microstructure on scales much smaller than that of the gridded wind fields used to drive our trajectory calculations. This microstructure of the tracer fields can easily attain a mesh size that is a full order of magnitude smaller than the $2.5° \times 2.5°$ mesh size of the gridded winds used in this study [as discussed in Pierrehumbert and Yang (1993)]. Such a nominally high resolution does not imply, however, that the fine 2D straining fields so obtained are accurate descriptions of the largely 3D physical processes that actually operate at the smallest length scales that we apparently resolve.

The resolution of the ECMWF model ($2.5° \times 2.5°$) from which our winds are derived is, in particular, not fine enough to resolve the eddies that contribute to the atmospheric energy cascade. Hence, the only contribution to puff dispersion is from the well-resolved flow fields on the scale of the 2D enstrophy cascade and larger scales. In other studies, random perturbations (Gifford 1988) or subgrid-scale diffusivities (Maryon and Buckland 1995) have been applied in order to account for the energy-cascade effects. The net effect of subgrid-scale diffusivity is not important, however, at the scales investigated here (Maryon and Buckland 1995). We have opted to neglect this effect in our integrations. Our dispersion over the long term is therefore slightly less than what explicit inclusion of finescale winds would produce, but we do not anticipate this to cause important qualitative differences.

In a sense, we have included the initial effect of subsynoptic-scale eddies, however, by making the initial puff distribution circular and of order of 1°; this is comparable to the state of a diffusing cloud at the point where the enstrophy cascade begins to dominate the dispersion process [e.g., Fig. 3 of Gifford (1988)]. We have performed extensive sensitivity studies increasing the diameter of the puff. As discussed in Er-El and Peskin (1981), Pierrehumbert and Yang (1993), and Babiano et al. (1990), the rate of dispersion is weakly affected by the initial scale of the release, leading us to choose the smallest scale that we can justify. Babiano et al. (1990) argue for a ratio of roughly 30 to 1 between the initial separation distance and σ_r to accurately cap-

ture either the RO or Kraichnan–Lin regimes. This requirement is satisfied in this study. Unless we adequately model the energy-cascade inertial range ($\sim<$200 km) well, there is nothing more to be gained by decreasing our initial separation distance further. Consequently, our sampling strategy is based on the initial puff being small enough to capture mixing by the finest resolved flow fields but not so small as to be in a regime in which the physical assumptions of our method break down (as discussed above).

Pierrehumbert and Yang (1993) computed finite-time Lyapunov exponents and found them to have extremely finescale structure. Trajectories initially 1° apart can have Lyapunov exponents differing by a factor of 5. Based on their work, we take 1° as an estimate of the minimum distance over which strong straining gradients occur. The puff scale should be of this order if we wish to differentiate between regions of high and low straining rates, that is, strongly and weakly chaotic regimes, respectively. As Pierrehumbert and Yang (1993) show, the low latitudes are characterized by broad stretches of small Lyapunov exponents, and the high latitudes display a patchier distribution of generally larger exponents. We may anticipate differences on short timescales between tropical and extratropical dispersion, which might be described as being due to variation in straining rates; hence, the puff size must be small enough to observe the dispersion within regions of homogeneous strain rates.

The timescale of puff release is dictated by the considerations above as well as by particle advection length scales estimated from typical wind values. For mean winds of 10 m s^{-1}, a 12-hourly injection of particles should produce a meaningful ensemble average, as ''overlapping'' of particles from one puff to the next is not likely to occur initially. Sensitivity studies (not shown) demonstrated little dependence of results on sampling frequency.

As pointed out by Maryon and Buckland (1995), a typical eddy turnover time τ can be rewritten for the exponential growth regime in a form analogous to an inverse Lyapunov exponent. The only difference is that the length of a material contour in the usual definition of a Lyapunov exponent is replaced by the rms particle separation, that is,

$$\lambda_{\sigma_r}(t, \sigma_r) = \frac{1}{t} \ln \frac{\sigma_{r(t)}}{\sigma_{r(t_0)}} = \tau^{-1}. \quad (6)$$

The Kraichnan–Lin exponential regime is expected to hold when the characteristic timescale τ of dispersing eddies is locally constant. Consequently, exponential growth can be expected for times comparable to an eddy-turnover time.

Two relevant eddy turnover times can be calculated. In the inertial subrange of the 2D or quasigeostrophic enstrophy cascade, the characteristic timescale τ can be estimated from the enstrophy cascade rate η as $\tau \approx \eta^{-1/3}$ (Kraichnan 1967; Leith 1968; Batchelor 1969; Lin 1972); by assuming a dependence of η on vorticity, this yields a timescale of $\sim 2\pi f^{-1}$ or about 0.5–2 days in midlatitudes (e.g., Gifford 1988). In the β-plane turbulence regime, the characteristic timescale τ equals $2\pi(U\beta_0)^{-1/2}$ (Charney 1955; Rhines 1975; Maltrud and Vallis 1991; Panetta 1993), where U is a characteristic zonal velocity and β_0 the local value of the meridional derivative of the Coriolis parameter. In this regime, we expect τ to also display latitudinal dependence. A typical midlatitude eddy-turnover time, calculated in this way, is about 0.5–3 days, but in the Tropics (making the equatorial β-plane assumption), it is roughly 3–8 days, given typical ranges of U and latitude. If these estimates of τ are accepted, then we may anticipate latitudinal variability in the distribution of exponential versus power-law dispersion growth.

In the EOLE study, balloons were released in clusters of three to four, the maximum number that could be tracked, every couple of hours, yielding an estimated initial separation of 150 km between clusters at typical winds of 20 m s^{-1}. TWERLE balloons were released about 30 min apart, with typical observed winds of 2–15 m s^{-1}, hence an initial separation between balloons of 5–30 km (Er-El and Peskin 1981). Thus, our sampling strategy differs from the strategies used in both the EOLE and TWERLE field experiments but is most similar to the latter in terms of individual particle spacing. The relatively large puff size and number of particles within a puff in our study should result in better sampling and more stable statistics than was possible in the field or in previous numerical studies.

The results we present are somewhat sensitive quantitatively, although not qualitatively, to the intervals over which they are calculated. Extensive studies of the sensitivity of our results to different sampling intervals show that little *systematic* bias is introduced when using a reasonable range of intervals, that is, varying the initial time considered from day 1 to 5 and the final time from day 7 to 15, and it is discussed below. We use therefore results from day 1 to 10 to study short-term relative dispersion.

4. Relative dispersion

The short-term dispersive behavior we see can be summarized as a combination of the superdiffusive power-law regime and the Kraichnan–Lin exponential-growth regime. As shown in Fig. 2, tropical dispersion over the initial 10 days is typically well fit by an exponential (dotted line in the figure). Extratropical releases encounter the strong shear-dispersion mechanism characteristic of synoptic-scale eddies (cf. Er-El and Peskin 1981) and hence are well fitted by the ballistic growth law or $\sigma_r \propto t^{1.0}$ (solid line). As shown in Fig. 2, a closer examination of rms particle separation in enhanced dispersion (open circles) regions reveals that the growth can be slow initially, after which it follows the RO power law, with $\gamma = 1.5$. The time-averaged

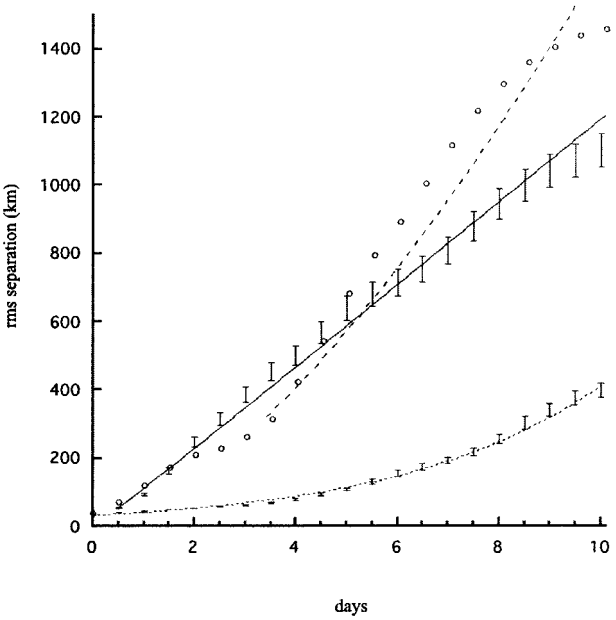

FIG. 2. Examples of rms puff size growth taken over an ensemble of puffs, as a function of time on the 315-K surface, for a typical tropical release (dotted line is curve fit) and two midlatitude releases (solid and dashed lines are the corresponding fits). The locations of the latter two releases are shown as squares in Fig. 4a (solid line from the Southern Hemisphere release, dashed line from the Northern Hemisphere). The midlatitude solid-line fit is ballistic ($\gamma = 1$); the release fitted with a dashed line has a higher power-law best fit over the whole 10-day interval ($\gamma = 1.2$), but this results from the inclusion of a slow initial phase and an RO ($\gamma = 1.5$) phase later (see text for more details). Data values for the latter case are shown as open circles whereas error bars only are shown for the former two releases for the sake of legibility (the data values fall in the middle of the error bars). Error was estimated as the ''standard error'' due to sampling. The locations of the power-law releases are indicated in Fig. 4.

winds shown in Fig. 3 are useful in this discussion and the section that follows.

An objective method to distinguish between the exponential and power-law regimes is to calculate power-law and exponential least squares fits and evaluate the regression coefficient R^2 of the fit. Any simple objective method such as this will not however, capture details of the dispersion's time evolution. Visual inspection of many curves like those in Fig. 2 (not shown) reveals, in some midlatitude cases, exponential growth for a short but significant time interval followed by power-law growth (Huber 1998). Sensitivity studies (not shown) indicate that no systematic errors arise by merely placing the results in two categories, the power-law regime and the exponential regime, based on relative goodness of fit. The average R^2 values for dispersion being fitted growth better by a power law were greater than 0.98 in all cases, the minimum R^2 for these cases was 0.925. For those releases better fitted by an exponential, the average R^2 is 0.98 and the minimum is 0.95. In nearly all cases, the difference in R^2 between the corresponding exponential and power-law fits was greater than or equal to the difference between average and minimum R^2 within either regime (discussed above).

In almost all cases, puff-size evolution for the regions within 15° of the equator is better fitted as an exponential for the first 10 days after puff release, while power-law behavior prevails in middle and high latitudes. The best power-law fits to the zonally averaged dispersion (within approximately 20° latitude bins) yield values of γ, which are nearly 1 in all seasons and regions (Table 1).

In the equatorial bins, the choice of interval over which to perform the best fit had some effect on the determination of power law versus exponential growth. The choice of fitting from day 1 to 10, made throughout this study, proved to generate marginal differences in R^2 between fits within the equatorial regions on the 330-K surface. A small change to fitting over an 8-day interval allows better discrimination via the difference in R^2 and reveals that the equatorial regions on the 330-K surface are unequivocally in the exponential-growth regime. In those regions in which the zonally averaged dispersion is best fitted as exponential, the mean value of τ is $\sim$4 days. The transition between regions that are best fitted by exponentials and those best fitted by power laws occurs roughly between 15° and 25° of the equator. As shown more clearly below, the separation between tropical and extratropical mixing regimes is sharper on the 315-K isentropic surface and less distinct on the 330-K surface. Discussion of the spatial and temporal variability of the dispersive behavior is carried out in the remainder of this section.

a. The power-law regime

Extratropical meridional dispersion is by and large superdiffusive regardless of height or season. The spatial variation of γ in those regions for which a power-law fit is better than an exponential one is shown in Fig. 4. A strong association of enhanced dispersion ($\gamma > 1$) with topography appears in the Northern Hemisphere during winter (warm colors in figure). Outside of these regions, the dispersion is roughly ballistic, with $\gamma \cong 1$ (green). The distribution of γ in the Southern Hemisphere is much more homogeneous, with values close to 1.0, although there are suggestions of enhancement over South America during the austral winter. The vertical coherence of γ demonstrates that particles beginning on the 315-K surface, even if carried diabatically to (or from) the 330-K surface, will experience substantially similar meridional dispersion (cf. Fig. 4a with 4b and Fig. 4c with 4d).

The spatial pattern of γ values in Fig. 4 points to the role of zonal inhomogeneities and the modulation of the trajectories by topography and storm tracks in determining the mixing characteristics on the timescale of interest. Trajectories that originate near topography and subsequently experience enhanced dispersion over their evolution in 1) the winter hemisphere and 2) near the storm tracks in the summer hemisphere suggest that

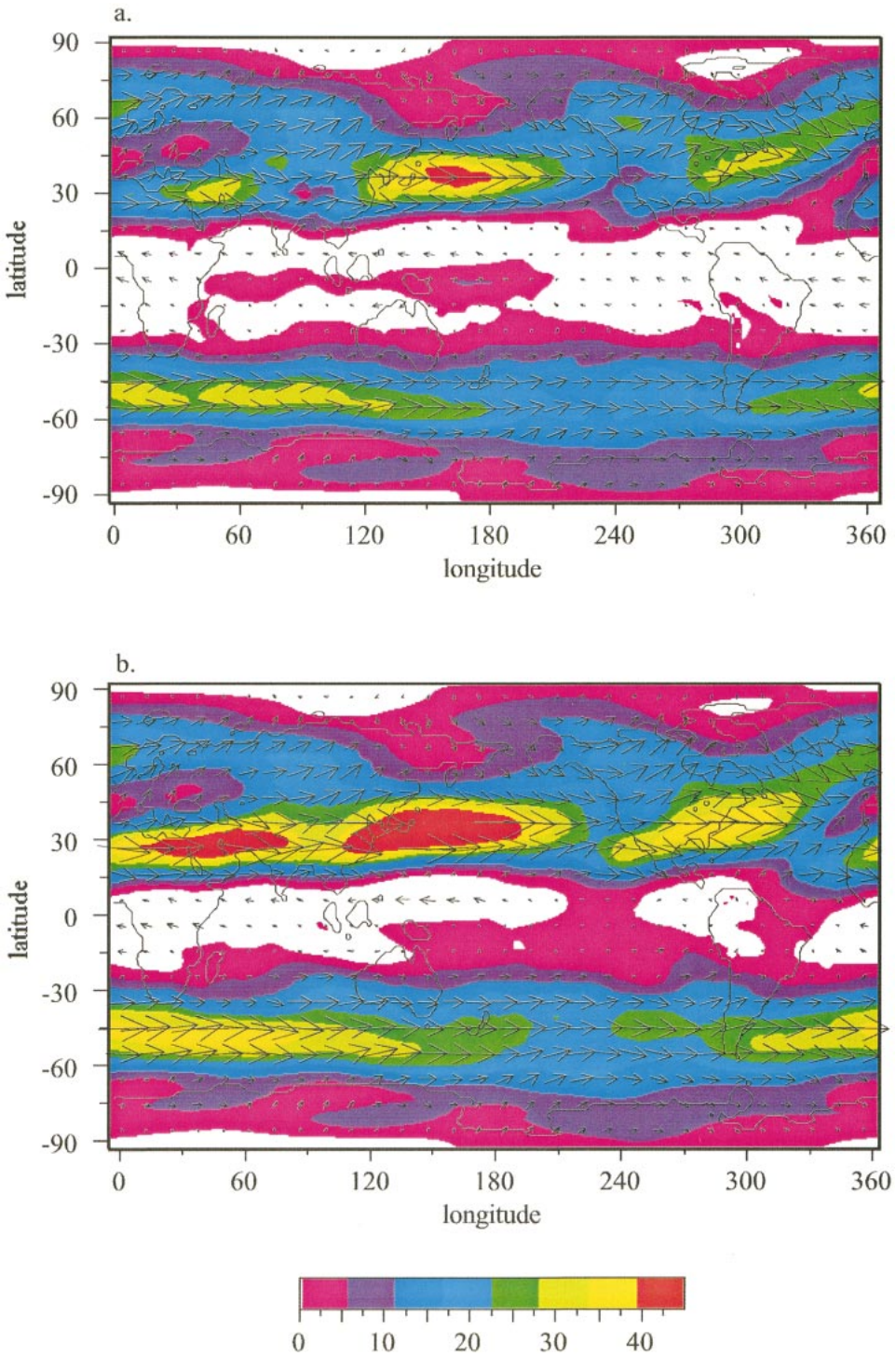

FIG. 3. Seasonal-average wind fields for the two extreme seasons, boreal (a), (b) winter and (c), (d) summer and the (a), (b) 315-K and (c), (d) 330-K isentropic surfaces. Vectors indicate wind direction and magnitude; the maximum length of vectors plotted is 45 m s^{-1}. Gaps in the vector plot indicate regions where the wind speed exceeds this maximum. The zonal wind magnitude is also plotted with a scale given by the color bar. Colors are suppressed for easterly winds (negative zonal winds in white).

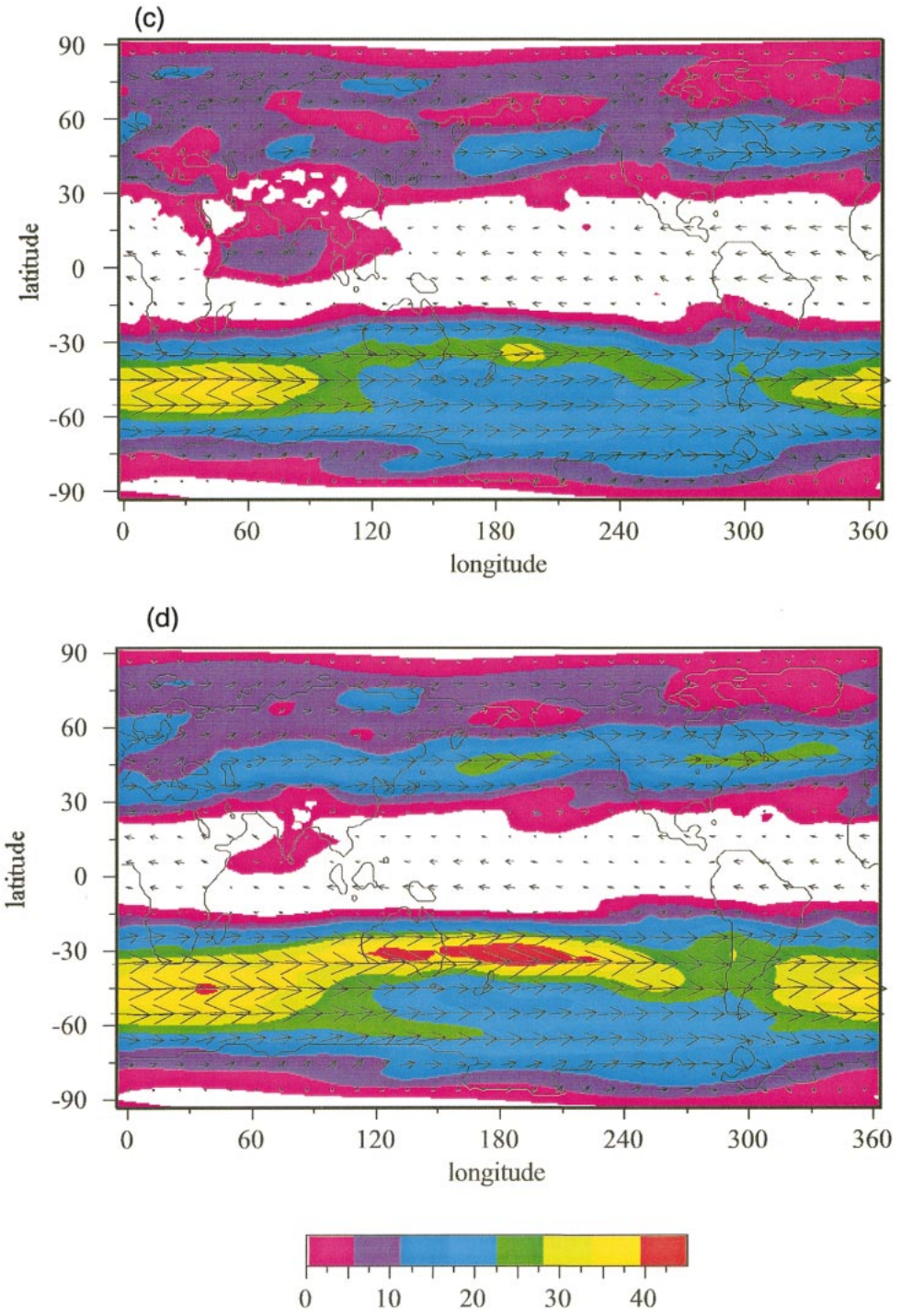

FIG. 3. (*Continued*)

irreversible mixing of PV as well as other tracers may be zonally focused to some extent. During boreal winter the largest values of γ are associated with puff releases close to and upstream of the Tibetan Plateau and the Rocky Mountains. Given mean zonal-flow velocities at these locations and the 10-day interval over which dispersion is measured, the plotted γ values reflect meridional dispersion about 50° east of the release locations.

We conjecture that two complementary effects are at play: 1) cross-streamline eddy-induced mixing in the jet streaks downstream of topography where streamlines merge and 2) chaotic mixing in the more quiescent but

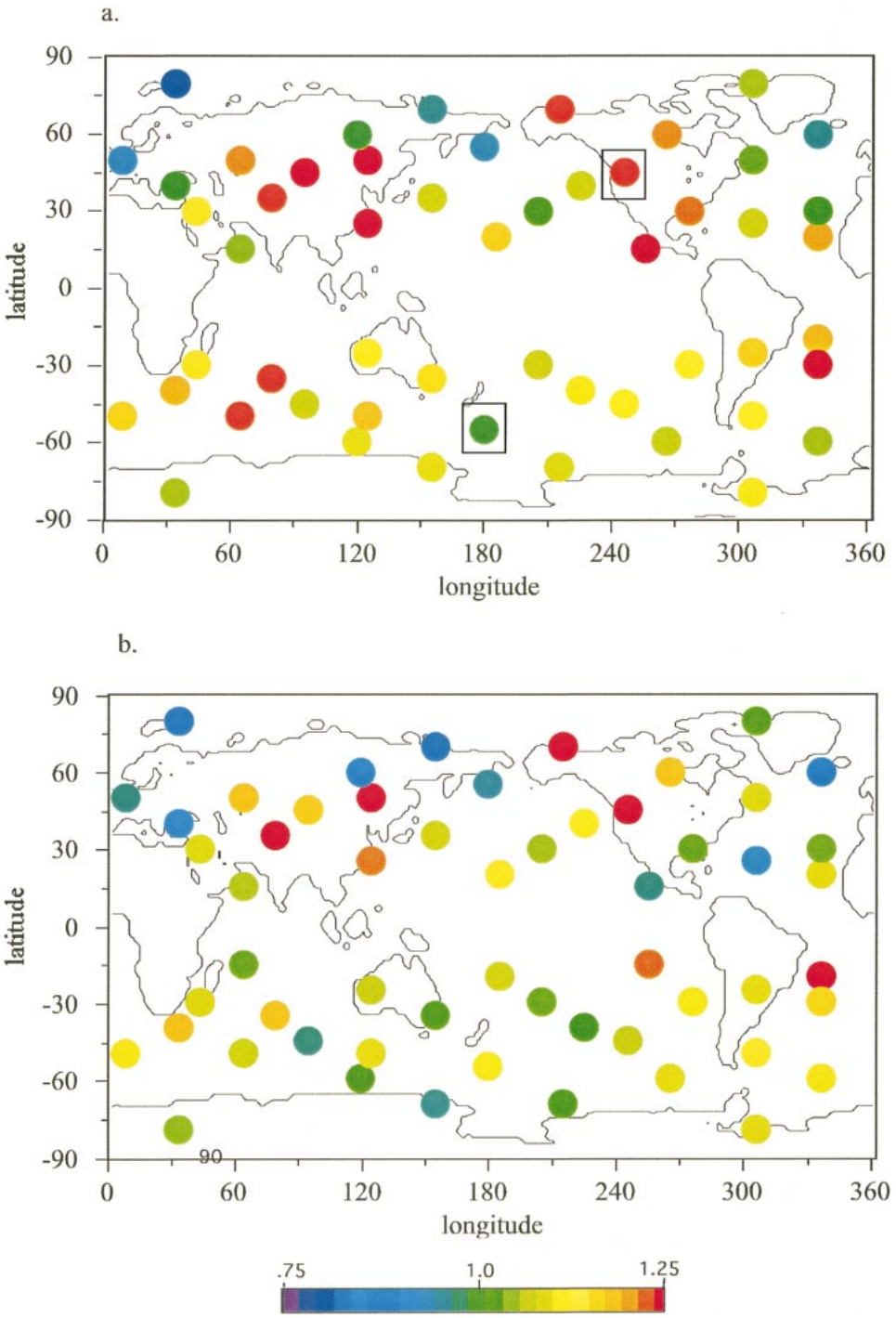

FIG. 4. Spatial distribution of the power-law exponent γ on (a), (c) the 315-K isentropic surface and (b), (d) the 330-K surface. The value of γ is determined from the best power-law fit (for those releases in which the best fit is a power law, see text) of the rms puff size as a function of time: (a), (b) boreal winter; (c), (d) boreal summer. The color bar indicates the value of γ. The circles are at the initial locations to which the value of γ is attributed (see text for details). In (e), γ is averaged over 330- and 315-K surfaces to minimize the effects of sampling variability and then interpolated onto a $10° \times 5°$ regular grid. We plot in green (boreal winter) and blue (boreal summer) regions in which the estimate of γ is more than 0.2 away from ballistic, that is, values of $\gamma < 0.8$ and $\gamma > 1.2$; these are values more than 3 std dev away from the value $\gamma = 1.0$. The initial location of the ballistic power-law release in Fig. 2 is indicated by a box in the Southern Hemisphere; the initial location of the RO release in Fig. 2 is indicated by a box in the Northern Hemisphere.

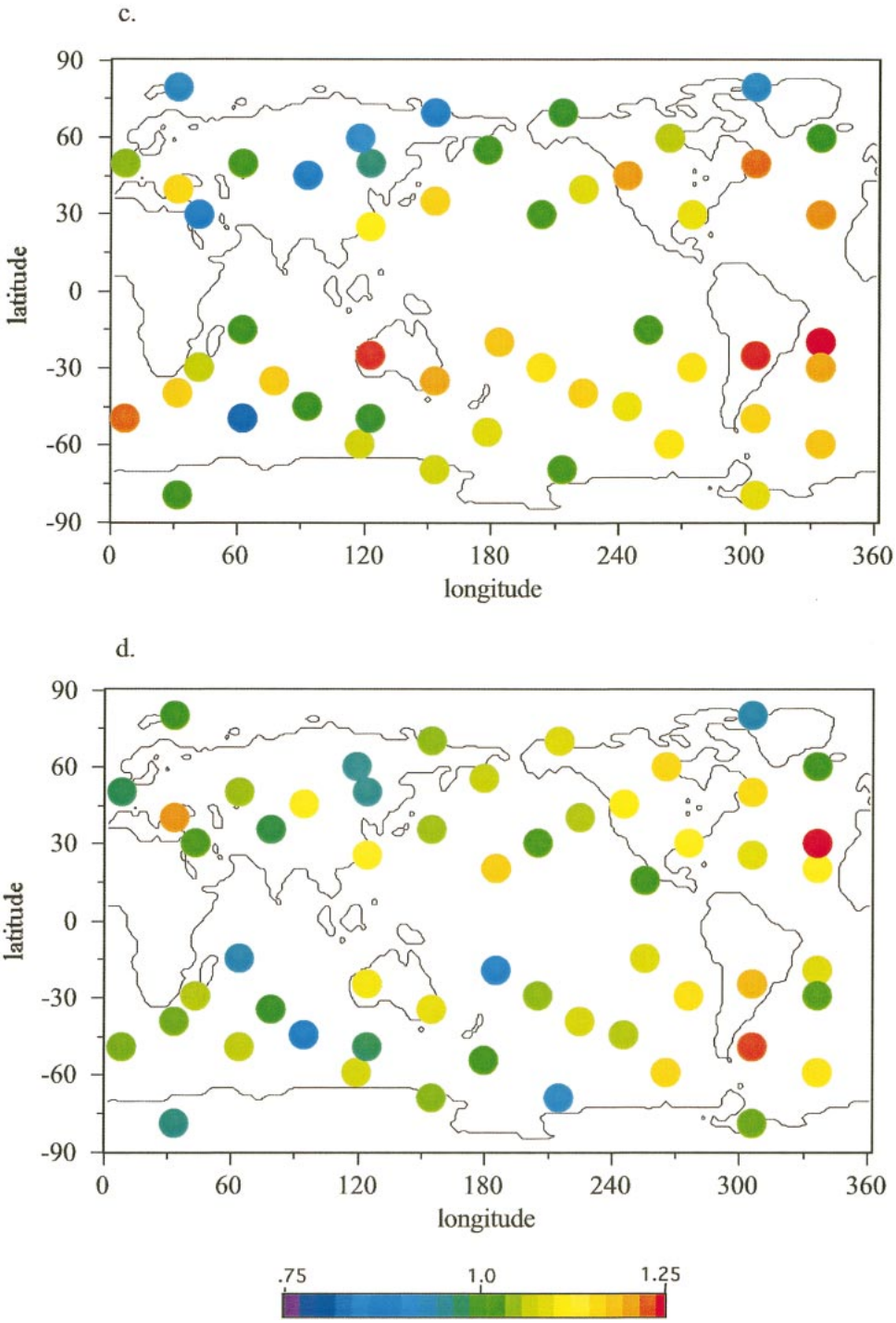

FIG. 4. (*Continued*)

diffluent flow upstream of and over topographic maxima. This pattern is consistent with recent theoretical work (Rom-Kedar et al. 1990; Pierrehumbert 1991a,b; Wiggins 1992; Yang 1996; Poje et al. 1999) that builds on classic results in dynamical systems theory (Poincaré 1899; Melnikov 1963; Smale 1967; Moser 1973) to demonstrate that in a frame of reference moving with a jet, the saddle-node dynamics associated with hyperbolic trajectories generates inhomogeneities in mixing characteristics.

Comparison between the two hemispheres provides no evidence of strong jets being correlated with reductions in the rate of dispersion, as has been suggested by the simplest theoretical considerations of jets as flow

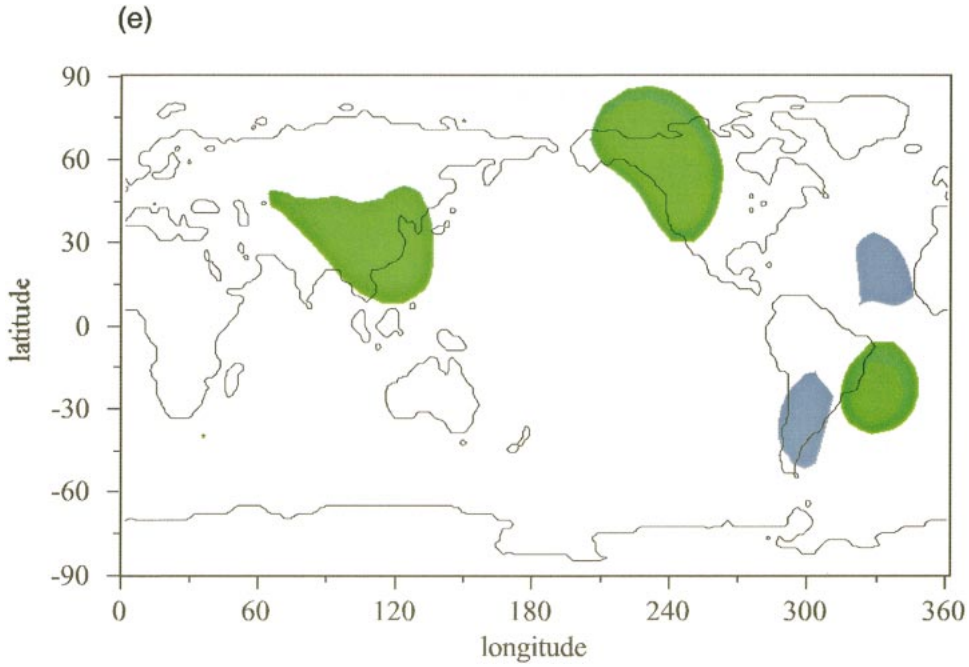

FIG. 4. (*Continued*)

separatrices. Other studies indicate that meandering jets may act both as barriers to cross-jet mixing or as vigorous agents of mixing on either side of the jet (e.g., Samelson 1996). The rough correlation of maxima of γ in the present study with maxima in eddy heat transport (Peixoto and Oort 1992) is striking in this context. Still, either one of these mechanisms is more likely to be important in a time-dependent fashion that is not amenable to the analysis we have performed here via comparison with time mean wind fields only. With due consideration of our analysis' limitations, comparison between seasons and heights reveals little correlation between time-average zonal-wind strength and meridional diffusivity reductions on short timescales (Fig. 5).

Furthermore, we find no support for the existence of subdiffusive behavior on these timescales, which is in keeping with previous work. The only significant deviation from purely ballistic behavior we can establish is enhanced (RO) mixing, found mostly in the Northern Hemisphere's winter, when the wave–trough pattern

TABLE 1. Values of the best fit power-law exponents γ in 20° latitude zonal belts centered at the latitude given in the leftmost corner. The term E indicates that the best fit is exponential, as described in the text.

Latitude	315 K winter	330 K winter	315 K summer	330 K summer
80	1.03	1.06	0.98	1.07
60	0.98	0.98	1.07	1.06
40	1.06	1.01	1.02	1.01
20	1.02	1.08	E	1.05
0	E	1.07* (E)	E	0.97* (E)
−20	1.14	1.14	1.18	1.09
−40	1.06	0.96	1.06	1.01
−60	1.06	1.09	1.12	1.06
−80	1.09	1.08	1.04	0.99

* Indicates that the value of this power-law exponent is sensitive to the choice of interval over which it is calculated: when the fit is performed over the initial 8 rather than 10 days, the best fit is exponential. See also Fig. 6 to justify our characterization of these regions as undergoing exponential dispersion growth.

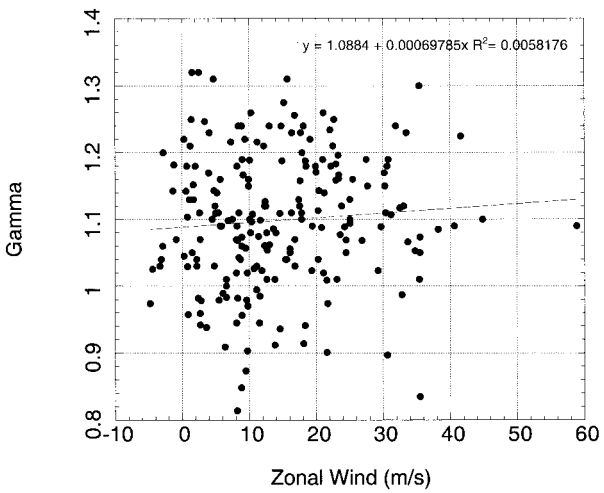

FIG. 5. The variation of the power-law exponent γ as a function of the zonal wind U. Values from all isentropic surfaces and seasons are included. For reference purposes, a linear regression through the values is supplied on the figure (note that the regression is not statistically significant). Analysis of the values stratified by season and hemisphere, as in Fig. 4, revealed neither any salient patterns nor regression results that had higher statistical significance.

there is most pronounced (Figs. 3, 4). This pattern of enhanced mixing is apparent in Fig. 4 in which γ values averaged over the 330- and 315-K surfaces are interpolated onto a regular grid. The interpolation was carried out by using statistically determined weights aimed at minimizing the variance of the estimate fields of missing data. This procedure is known as ''kriging'' in mathematical geology [see Handcock and Wallis (1994) along with associated discussant papers and references therein] and as ''optimal interpolation'' in the meteorological (Daley 1991) and oceanographic (Ghil and Malanotte-Rizzoli 1991) literature. The implementation of this procedure used a spherical model of spatial distribution and 100 passes to minimize the variance of the missing γ values on the regular grid [using the Fortner transform package, Fortner (1996)].

From the results in Fig. 4e, it is clear that some regions have consistently large deviations from ballistic behavior. These spatially coherent deviations (shown as green and blue patches in the figure) are, in fact, all above $\gamma = 1.2$. We note that these patches, in which releases of puffs of passive tracers will tend to separate meridionally more over the course of the puff evolution than those released from most other regions, are associated by and large with major mountain ranges or upstream of the storm tracks. However, the limitations of the methods as we have applied them in this study do not allow us to do more than conjecture as to the cause of this pattern.

b. The Kraichnan–Lin exponential regime

In Fig. 6, we show the spatial variation of τ for dispersion growth that is better fitted by an exponential over at least 10 days. The regions of exponential dispersion growth are essentially limited to the tropical easterlies. This is consistent with the homogeneous band of small finite-time Lyapunov exponents calculated by Pierrehumbert and Yang (1993) and their characterization of this band as a region of ''weak chaos.'' In fact, as discussed in section 3c, τ may be interpreted as an inverse Lyapunov exponent. The values shown in Fig. 6, while about half those found in midlatitudes by Pierrehumbert and Yang (1993) and Maryon and Buckland (1995), are comparable with those for tropical releases in Pierrehumbert and Yang (1993). The average value of τ for all the cases is 3.6 days, and the probability density function of τ (not shown) is suggestive of a normal distribution; more samples would be required, however, to establish this firmly. Thus, a typical eddy turnover time from this analysis is about 4 days, in keeping with the theoretical estimates discussed in the previous section. Recently independent estimates of dispersion in a tropical monsoonlike flow using very different methods described in Joseph and Moustaoui (2000) calculated a characteristic timescale of 3.6 days [fortuitously close to the estimate here and to Huber (1998)], which we consider to be validation of the robustness of this estimate.

Breaks in the easterlies (as in Figs. 3 and 6) in boreal winter are due to the sporadic intrusion of westerlies, whereas the boreal summer fields are influenced by the Asian monsoon. The highest values of τ, corresponding to a fairly short turnover time of about 2 days, are found mostly at the fringes of the easterlies, where 1) transport across the equator and into midlatitudes is more likely to occur and 2) wave breaking may be playing a role (Waugh et al. 1994; Rom-Kedar et al. 1997). The highest values are attained during boreal winter, in the upper troposphere (Fig. 6b), near breaks in the easterlies in the central Pacific, and over Brazil. By comparison, the boreal-summer easterlies are fairly homogeneous zonally and the *e*-folding time remains high (Figs. 6c, d).

5. Summary

We have analyzed the meridional mixing of passive tracers produced by realistic ECMWF wind fields (Fig. 3) interpolated onto isentropic surfaces (Fig. 1). The spatial pattern and the timescale of transitions from one mode of growth to another reveal a number of important details that have not been described previously. The atmospheric mixing displays a wealth of patterns indicative of anomalous dispersion in a chaotic fluid (e.g., Rom-Kedar and Paldor 1997; Weiss et al. 1998). By examining the dependence of the large-scale mixing on isentropic surface, season, and horizontal location, we have assessed the relevance of various simpler or more specialized theories of mixing in geophysical fluids.

For the relatively short timescale selected here (1–10 days), the mixing regimes suggested by theoretical arguments are seen to fall within geographically coherent regions with only slight dependence on height. Dependence of the dispersion on the seasonal cycle is limited except for what we interpret as the indirect effect of seasonal changes in the flow's zonal inhomogeneities (Fig. 4). There is little correlation between the dispersive regimes and the seasonal evolution (or hemispheric variation) of seasonally averaged jet stream strength (Fig. 5).

Extratropical meridional dispersion on these short timescales is generally well characterized as being of power-law type [cf. Eq. (3)] and superdiffusive. This dispersion behavior is consistent with the nonlocal character of midlatitude mixing. Typically, $\gamma \cong 1$, that is, this superdiffusive dispersion is roughly ballistic (Table 1). On closer inspection, there are zonally localized regions of even more enhanced dispersion.

We take the presence of greater than ballistic growth, with $\gamma \approx 1.5$, that is, approximately following the RO law, to indicate that puffs encounter larger and larger eddies and enhanced mixing due to changes in the flow trajectories, probably related to planetary wave or storm track activity. This spatial pattern suggests that consideration of the streamline geometry may be important in

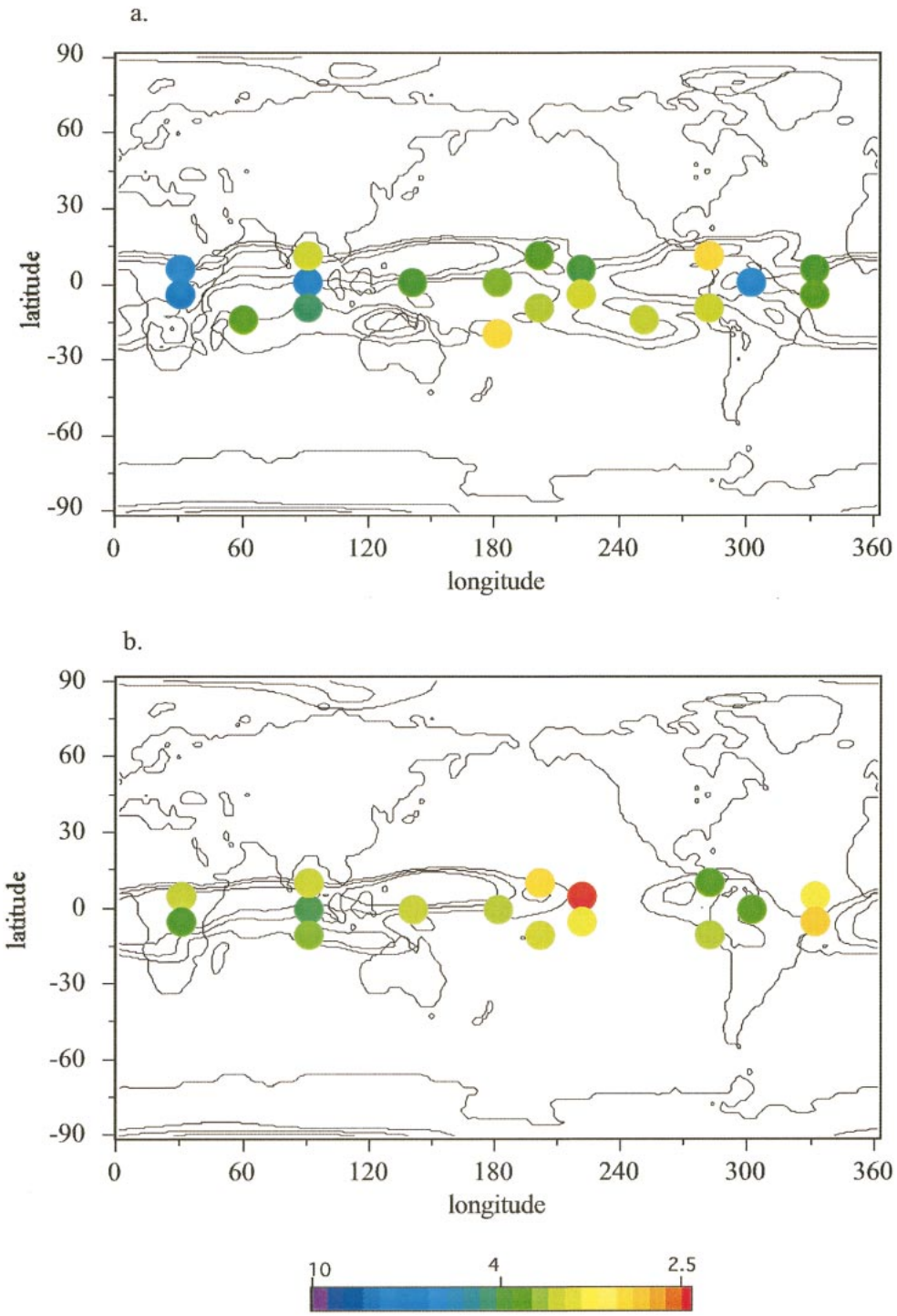

FIG. 6. The spatial variation of the characteristic timescale τ for short-term dispersion in the Tropics. The value of τ is determined from the best exponential fit (for those releases in which the best fit is an exponential; see text for details) of the rms puff size as a function of time: (a), (b) boreal winter; (c), (d) boreal summer. Color bar indicates value of τ; thus, green corresponds to an eddy turnover time value of 4 days. The 0, 2, and 4 m s^{-1} easterly winds are contoured on (a), (c) the 315-K and (b), (d) the 330-K surfaces.

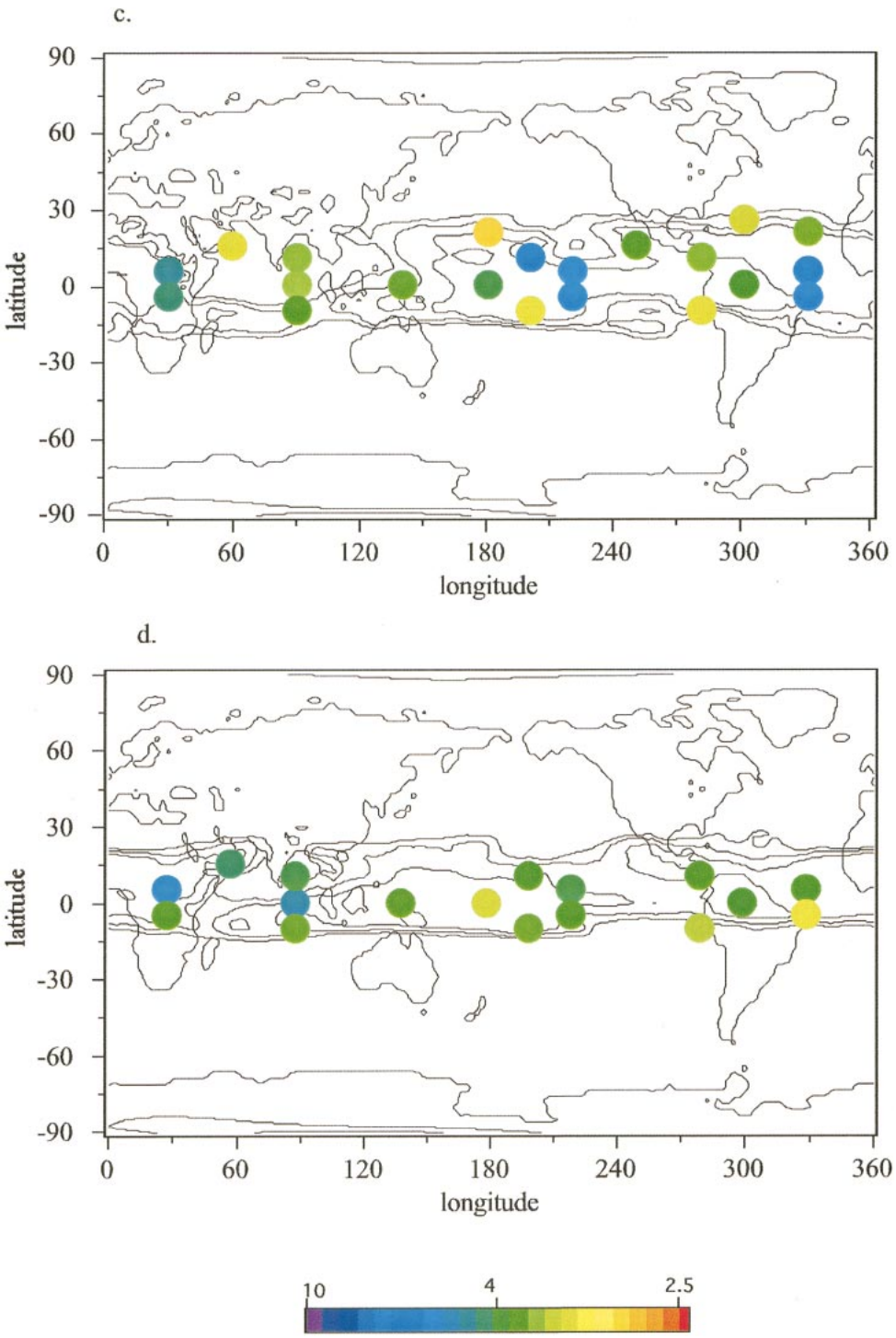

FIG. 6. (*Continued*)

understanding enhanced meridional mixing (Fig. 4), but the analysis performed here cannot tease apart the relative roles of planetary waves, storm tracks, or other possible mechanisms.

Having found a fairly wide range of γ values (Fig. 5) allows us to reconcile the fact that previous studies have given evidence for both ballistic and RO laws. The present study provides evidence that the RO and ballistic laws may both be valid on the (fixed) timescale of interest here. Consequently, tracers released from different initial locations and seasons might sample either regime.

Preliminary examination of longer timescales sug-

gests a spatially varying blend of subdiffusive, diffusive, ballistic, and RO regimes, as described in Huber (1998). If time were normalized to the characteristic Lagrangian velocities of the flow, we expect that a more uniform transition between distinct dispersion regimes, from exponential at very short times to superdiffusive intermediate times and eventually to diffusive and subdiffusive, might be found (e.g., Artale et al. 1997; Huber 1998).

Within the Tropics, exponential growth of the dispersion is a better fit to the data than power-law growth. This is consistent with the latitudinal dependence of the characteristic eddy timescales discussed above. The Kraichnan–Lin exponential growth regime's prevailing in the Tropics is consistent with the presence of homogeneous and relatively slow Lagrangian timescales that are encountered by growing puffs. This regime is found, at closer inspection, to correspond roughly with the tropical easterlies (Fig. 6). In those regions where westerlies intrude and tropical wave breaking is thought to occur, the exponential regime less distinct and replaced phases of power-law growth. The geographic separation between the exponential and power-law regimes indicates that the relative dispersion we estimated here does capture the presence of a tropical–extratropical barrier to transport, although it is expressed in a different form than usual (e.g., Yang 1995; Huber 1998). This barrier separates the slowly dispersing, weakly chaotic easterly Tropics from the highly dispersive, more strongly chaotic westerly extratropics.

We can draw the following conclusions from this analysis.

- Dispersive behavior is substantially similar on the 315- and 330-K isentropic surfaces.
- The Kraichnan–Lin exponential growth law is a quantitatively better fit to the dispersion data than any power law in the tropical belt of easterlies over the timescale considered.
- In mid- to high latitudes, power-law growth is the better fit. In general, the value of the power-law exponent γ equals approximately 1; therefore, extratropical dispersion on timescales less than 10 days is best characterized as ballistic.
- The separation of power-law and Kraichnan–Lin regimes is consistent with the presence of a tropical–extratropical barrier to transport between easterly and westerly winds.
- The zonal average of γ is not substantially affected by seasonal changes and associated variations in zonal-mean wind speed.
- There is, however, a range of γ, from $\sim$0.8 to $\sim$1.3, within which larger values of γ are associated with the seasonal-mean, ridge–trough circulation patterns; in particular, we conjecture that stationary waves in the Northern Hemisphere's winter and enhanced eddy activity in the storm tracks might produce these larger γ values.
- In the regions that experience enhanced dispersion growth, γ equals approximately 1.5, that is, the RO law, from day 2–3 to day 7–10.

Tropospheric meridional dispersion on timescales less than 10 days is thus well described as being in the intermediate turbulence regime in which coherent structures play an important role in determining overall mixing behavior (e.g., Poje et al. 1999). Consequently, theoretical treatments and parameterizations of meridional mixing that rely on the eddy diffusion approximation are ill-suited to represent dispersion on these timescales. It is important to describe theoretically the effects of coherent structures on turbulent flows in order to formulate better parameterizations of heat, momentum, and tracer transport by atmospheric turbulence, from the mesoscale up to hemispheric scales.

Acknowledgments. It is a pleasure to acknowledge helpful discussions with B. L. Hua, K. Ide, B. Legras, N. Paldor, R. T. Pierrehumbert, V. Rom-Kedar, S. Smith, K. Swanson, G. Vallis, S. Wiggins, H. Yang, and N. Zeng. Constructive comments from three anonymous reviewers helped improve the presentation and clarity of ideas This work benefited from support by ATM96-23787 at UCLA and ATM98-781099 at UCSC (MH), ONR N00014-98-1-0165 (JCM), and an NSF Special Creativity Award (MG). MH is extremely grateful to MG and JCM, who advised him throughout his master's thesis research, of which this study is a part, and also many informative discussions with others at UCLA. MH also is grateful to L. C. Sloan for support while continuing this work. This is publication number 5497 of UCLA's Institute of Geophysical and Planetary Physics.

REFERENCES

Aref, H., 1983: Integrable, chaotic, and turbulent vortex motion in two-dimensional flows. *Ann. Rev. Fluid Mech.,* **15,** 345–389.

——, 1991: Stochastic particle motion in laminar flows. *Phys. Fluids,* **3A,** 1009–1016.

Artale, V., G. Boffetta, A. Celani, M. Cencini, and A. Vulpiani, 1997: Dispersion of passive tracers in closed basins: Beyond the diffusion coefficient. *Phys. Fluids,* **9,** 3162–3171.

Babiano, A., C. Basdevant, P. Le Roy, and R. Sadourny, 1990: Relative dispersion in two-dimensional turbulence. *J. Fluid Mech.,* **214,** 535–557.

——, G. Boffetta, A. Provenzale, and A. Vulpiani, 1994: Chaotic advection in point vortex models and 2-dimensional turbulence. *Phys. Fluids,* **7A,** 2465–2474.

Basdevant, C., B. Legras, R. Sadourny, and M. Beland, 1981: A study of barotropic model flows: Intermittency, waves and predictability. *J. Atmos. Sci.,* **38,** 2305–2326.

Batchelor, G. K., 1952: Diffusion in a field of homogeneous turbulence: The relative motion of particles. *Proc. Cambridge Philos. Soc.,* **48,** 345–362.

——, 1969: Computation of the energy spectrum in homogeneous two-dimensional turbulence. *Phys. Fluids,* **12,** 233–239.

Behringer, R. P., S. D. Meyers, and H. L. Swinney, 1991: Chaos and mixing in a geostrophic flow. *Phys. Fluids,* **3A,** 1243–1249.

Boffetta, G., V. Rago, and A. Celani, 1997: Transient anomalous dispersion in random walkers. *Phys. Lett.,* **235A,** 15–18.

Cardoso, O., B. Gluckmann, O. Parcollet, and P. Tabeling, 1996:

Dispersion in a quasi-two-dimensional-turbulent flow: An experimental study. *Phys. Fluids*, **8,** 209–214.
Charney, J. G., 1955: The Gulf Stream as an inertial boundary layer. *Proc. Natl. Acad. Sci.,* **41,** 731–740.
——, 1971: Geostrophic turbulence. *J. Atmos. Sci.,* **28,** 1087–1095.
Chen, P., 1995: Isentropic cross-tropopause mass exchange in the extratropics. *J. Geophys. Res.,* **100,** 16 661–16 673.
Daley, R., 1991: *Atmospheric Data Analysis.* Cambridge University Press, 457 pp.
del-Castillo-Negrete, D., 1998: Asymmetric transport and non-Gaussian statistics of passive scalars in vortices in shear. *Phys. Fluids,* **10,** 576–594.
Er-El, J., and R. L. Peskin, 1981: Relative diffusion of constant-level balloons in the Southern Hemisphere. *J. Atmos. Sci.,* **38,** 2264–2274.
Fjørtoft, R., 1953: On the changes in the spectral distribution of kinetic energy for two-dimensional, non-divergent flow. *Tellus,* **3,** 225–230.
Fortner Research LLC, 1996: Fortner Transform User's Guide, 310 pp.
Frisch, U., 1995: *Turbulence: The Legacy of A. N. Kolmogorov.* Cambridge University Press, 310 pp.
Ghil, M., and P. Malanotte-Rizzoli, 1991: Data assimilation in meteorology and oceanography. *Advances in Geophysics,* Vol. 33, Academic Press, 141–266.
Gifford, F. A., 1988: A similarity theory of the tropospheric turbulence energy spectrum. *J. Atmos. Sci.,* **45,** 1370–1379.
Handcock, M. S., and J. R. Wallis, 1994: An approach to statistical spatial-temporal modeling of meteorological fields. *J. Amer. Stat. Assoc.,* **89,** 368–390.
Haynes, P. H., and M. E. McIntyre, 1987: On the evolution of vorticity and potential vorticity in the presence of diabatic heating and frictional or other forces. *J. Atmos. Sci.,* **44,** 828–841.
Held, I. M., 1999: The macroturbulence of the troposphere. *Tellus,* **51A,** 59–70.
Hoskins, B. J., 1991: Towards a PV-θ view of the general circulation. *Tellus,* **43,** 27–37.
Huber, M., 1998: A Lagrangian investigation of large-scale atmospheric turbulence. M.S. thesis, Atmospheric Sciences Dept., University of California, Los Angeles, 47 pp. [Available from M. Huber, Earth Sciences Dept., University of California, Santa Cruz, Santa Cruz, CA 95064.]
Jones, S., 1991: The enhancement of mixing by chaotic advection. *Phys. Fluids,* **3A,** 1081–1086.
Joseph, B., and M. Moustaoui, 2000: Transport, moisture, and rain in a simple monsoonlike flow. *J. Atmos. Sci.,* **11,** 1817–1838.
Joussaume, S., and J. Jouzel, 1993: Paleoclimatic tracers: An investigation using an atmospheric General Circulation Model under Ice Age conditions 2. Water isotopes. *J. Geophys. Res.,* **98,** 2807–2830.
Julian, P., W. Massman, and N. Levanon, 1977: The TWERLE experiment. *Bull. Amer. Meteor. Soc.,* **58,** 936–948.
Kelly, K. K., A. F. Tuck, and T. Davies, 1991: Wintertime asymmetry of upper tropospheric water between the Northern and Southern Hemispheres. *Nature,* **353,** 244–247.
Klafter, J., M. F. Shlesinger, and G. Zumofen, 1996: Beyond Brownian motion. *Phys. Today,* **49,** 33–35.
Kraichnan, R. H., 1967: Inertial ranges in two-dimensional turbulence. *Phys. Fluids,* **10,** 1417–1423.
Leith, C. E., 1968: Diffusion approximation for two-dimensional turbulence. *Phys. Fluids,* **11,** 671–673.
Leovy, C. B., C. R. Sun, M. H. Hitchman, E. E. Rembsberg, J. M. Russell, L. L. Gordley, J. C. Gille, and L. V. Lyjak, 1985: Transport of ozone in the middle stratosphere: Evidence for planetary wave breaking. *J. Atmos. Sci.,* **42,** 230–242.
Lin, J., 1972: Relative dispersion in the enstrophy-cascading inertial range of homogeneous two-dimensional turbulence. *J. Atmos. Sci.,* **29,** 394–396.
Maltrud, M. E., and G. K. Vallis, 1991: Energy spectra and coherent structures in forced two-dimensional and beta-plane turbulence. *J. Fluid Mech.,* **228,** 321–342.
Maryon, R. H. and A. T. Buckland, 1995: Tropospheric dispersion: The first ten days after a puff release. *Quart. J. Roy. Meteor. Soc.,* **121,** 1799–1833.
McWilliams, J. C., 1984: The emergence of coherent vortices in turbulent flow. *J. Fluid Mech.,* **146,** 21–43.
Melnikov, V., 1963: On the stability of the center for time-periodic perturbations. *Trans. Moscow Math. Soc.,* **12,** 1–57.
Merril, J. T., R. Bleck, and D. Boudra, 1986: Techniques of Lagrangian trajectory analysis in isentropic coordinates. *Mon. Wea. Rev.,* **114,** 571–581.
Mezic, I., and S. Wiggins, 1994: On the dynamical origin of asymptotic t^2 dispersion of a nondiffusive tracer in incompressible laminar flows. *Phys. Fluids,* **6,** 2227–2229.
Morel, P., and W. Bandeen, 1973: The EOLE experiment: Early results and current objectives. *Bull. Amer. Meteor. Soc.,* **54,** 298–305.
——, and M. Larchevêque, 1974: Relative dispersion of constant-level balloons in the 200 mb general circulation. *J. Atmos. Sci.,* **31,** 2189–2196.
Moser, J., 1973: *Stable and Random Motions in Dynamical Systems.* Princeton University Press, 198 pp.
Nastrom, G., and K. Gage, 1985: A climatology of atmospheric wavenumber spectra of wind and temperature observed by commercial aircraft. *J. Atmos. Sci.,* **42,** 950–960.
Panetta, R. L., 1993: Zonal jets in wide baroclinically unstable regions: Persistence and scale selection. *J. Atmos. Sci.,* **50,** 2073–2106.
Peixoto, J. P., and A. H. Oort, 1992: *Physics of Climate.* AIP, 520 pp.
Pierrehumbert, R. T., 1991a: Chaotic mixing of tracer and vorticity by modulated traveling Rossby waves. *Geophys. Astrophys. Fluid Dyn.,* **58,** 285–319.
——, 1991b: Large-scale horizontal mixing in planetary atmospheres. *Phys. Fluids,* **3A,** 1250–1260.
——, 1998: Lateral mixing as a source of subtropical water vapor. *Geophys. Res. Lett.,* **25,** 151–154.
——, and H. Yang, 1993: Global chaotic mixing on isentropic surfaces. *J. Atmos. Sci.,* **50,** 2462–2480.
Poincaré, H., 1899: *Les Methodes Nouvelles de la Mécanique Céleste.* Gauthier-Villars, 283 pp.
Poje, A. C., G. Haller, and I. Mezic, 1999: The geometry and statistics of mixing in aperiodic flows. *Phys. Fluids,* **11,** 2963–2968.
Provenzale, A., 1999: Transport by coherent barotropic vortices. *Ann. Rev. Fluid Mech.,* **31,** 55–93.
——, A. Babiano, and B. Villone, 1995: Single-particle trajectories in 2-dimensional turbulence. *Chaos Solitons Fractals,* **5,** 2055–2071.
Rhines, P. B., 1975: Waves and turbulence on the beta-plane. *J. Fluid. Mech.,* **69,** 417–443.
Richardson, L. F., 1926: Atmospheric diffusion shown on a distance-neighbor graph. *Proc. Roy. Soc. London,* **110A,** 709–737.
——, and H. Stommel, 1948: Note on eddy diffusion in the sea. *J. Meteor.,* **5,** 238–240.
Rom-Kedar, V., and N. Paldor, 1997: From the Tropics to the poles in forty days. *Bull. Amer. Meteor. Soc.,* **78,** 2779–2784.
——, A. Leonard, and S. Wiggins, 1990: An analytical study of transport, mixing, and chaos in an unsteady vortical flow. *J. Fluid Mech.,* **214,** 347–394.
——, Y. Dvorkin, and N. Paldor, 1997: Chaotic Hamiltonian dynamics of particle's horizontal motion in the atmosphere. *Physica,* **106D,** 389–431.
Seo, K.-H., and K. P. Bowman, 2000: Lévy flights and anomalous diffusion in the stratosphere. *J. Geophys. Res.,* **10,** 12 295–12 302.
Sherwood, S., 1996: Maintenance of the free-tropospheric tropical water vapor distribution. Part 2: Simulation by large-scale advection. *J. Climate,* **9,** 2919–2934.
Shlesinger, M. F., G. M. Zaslavsky, and J. Klafter, 1993: Strange kinetics. *Nature,* **363,** 31–34.

Smale, S., 1967: Differentiable dynamical systems. *Bull. Amer. Math. Soc.,* **73,** 747–817.

Solomon, T. H., E. R. Weeks, and H. L. Swinney, 1994: Chaotic advection in a two-dimensional flow: Levy flights and anomalous diffusion. *Physica,* **76D,** 70–84.

Thiébaux, M. L., 1976: One-particle, two-dimensional effective eddy diffusivities from balloon trajectories. *J. Atmos. Sci.,* **33,** 1050–1059.

Waugh, D. W., L. M. Polvani, and R. A. Plumb, 1994: Nonlinear, barotropic response to a localized topographic forcing: Formation of a ''tropical surf zone'' and its effect on interhemispheric propagation. *J. Atmos. Sci.,* **51,** 1401–1416.

Weiss, J. B., 1991: Transport and mixing in traveling waves. *Phys. Fluids,* **3A,** 1379–1384.

——, A. Provenzale, and J. C. McWilliams, 1998: Lagrangian dynamics in high-dimensional point-vortex systems. *Phys. Fluids,* **10A,** 1929–1941.

Wiggins, S., 1992: *Chaotic Transport in Dynamical Systems.* Springer, 301 pp.

Yang, H., 1995: Three-dimensional transport of the Ertel potential vorticity and N_2O in the GFDL SHYHI model. *J. Atmos. Sci.,* **52,** 1513–1528.

——, 1996: Chaotic transport and mixing by ocean gyre circulation. *Stochastic Modeling in Physical Oceanography,* R. Adler, P. Müller, and B. Rozovskii, Birkhäuser, 115–130.

——, and R. T. Pierrehumbert, 1994: Production of dry air by isentropic mixing. *J. Atmos. Sci.,* **51,** 3437–3454.

Young, W. R., and S. Jones, 1991: Shear dispersion. The enhancement of mixing by chaotic advection. *Phys. Fluids,* **3A,** 1087–1101.